miR-95 promotes osteosarcoma growth by targeting *SCNN1A*

YANNAN GENG[1*], SHAORONG ZHAO[2*], YUTAO JIA[1], GANG XIA[1], HUIMING LI[1], ZHAO FANG[1], QUAN ZHANG[1] and RONG TIAN[1]

[1]Department of Spinal Surgery, Tianjin Union Medical Center, Tianjin 300121;
[2]The 3rd Department of Breast Cancer, China Tianjin Breast Cancer Prevention, Treatment and Research Center, Tianjin Medical University Cancer Institute and Hospital, National Clinical Research Center of Cancer, Tianjin 300060, P.R. China

Received July 31, 2019; Accepted January 21, 2020

DOI: 10.3892/or.2020.7514

Abstract. Osteosarcoma (OS) is a common malignant bone tumor, presenting particularly in children and young adults, and accounts for approximately 19% of all malignant bone cancers. Despite advances in OS treatment, long-term prognosis remains poor. miRNAs are non-coding single-stranded RNAs ~22 nucleotides in length. Increasing evidence suggests that numerous miRNAs may play critical roles in tumorigenesis and tumor progression; however, the role of miR-95 in OS has not been examined. In the present study, we investigated the role of miR-95 in OS using *in vitro* and *in vivo* models and publicly available expression data. Our findings indicate that abnormal miR-95 expression occurs in OS, according to the Gene Expression Omnibus (GEO) database. The miR-95 inhibitor reduced cell proliferation and promoted apoptosis in OS cell lines as detected by EdU staining, TUNEL staining and flow cytometry. Furthermore, a dual luciferase reporter assay revealed that miR-95 regulates the cell cycle of OS cells and apoptosis by targeting sodium channel epithelial 1α subunit (*SCNN1A*). Additionally, miR-95 antagomir suppressed the growth of U2OS xenograft tumors in a mouse model. In summary, our results suggest that miR-95 induces OS growth *in vitro* and *in vivo* by targeting *SCNN1A*. Our results help clarify the mechanism underlying the miR-95-mediated effects on OS tumor growth, thus potentially establishing it as a diagnostic target.

Introduction

Osteosarcoma (OS) is a common malignant bone tumor, presenting especially in children and young adults, accounting for approximately 19% of all cases of malignant bone cancers (1). Despite advancements in OS treatment, including surgery, chemotherapy, and radiotherapy, the long-term prognosis remains poor (2,3). Therefore, it is necessary to identify reliable, noninvasive biologic markers to monitor OS and its progression and to assess the response to therapy.

miRNAs are non-coding single-stranded RNAs of ~22 nucleotides in length. miRNAs downregulate approximately one-third of mammalian protein-coding mRNAs through mRNA degradation and/or translational suppression (4). Increasing evidence indicates that numerous miRNAs play critical roles in tumorigenesis and tumor progression (5,6).

Certain miRNAs are crucial oncogenes or tumor suppressors in OS. miR-17, miR-214, and miR-18a-5p are upregulated in OS and contribute to tumor growth (7-9), while miR-423-5p, miR-491-5p, and miR-590-3p are downregulated and function as tumor suppressors (10-12). Differences in expression profiles between non-neoplastic and OS tissues can partially elucidate the functions of miRNAs in tumorigenesis. Previous studies have suggested that miR-95 has distinct expression profiles in different types of cancers, including hepatoma, lung cancer, and colorectal cancer (13-15). However, the function of miR-95 in OS is unknown.

The present study aimed to investigate the role of miR-95 in OS using *in vitro* and *in vivo* models and publicly available expression data. Our results may help clarify the mechanism underlying the miR-95-mediated effects on OS tumor growth, thus potentially establishing it as a diagnostic target.

Materials and methods

Cell culture and transfection. Human OS cell lines U2OS, MG-63, and Saos-2 were obtained from the American Type Culture Collection (ATCC). Cells were cultured in DMEM containing 10% FBS and 100 U/ml penicillin/streptomycin (TransGen) at 37˚C and 5% CO_2. The miR-95 inhibitor, miR-95 mimics, miR-95 antagomir, miR-499a-5p inhibitor, and miRNA negative control (NC) were purchased from Ribo Co. (Kunshan, China). The mimics, inhibitor, and negative control were used to transfect OS cells with Lipofectamine 2000 (Invitrogen; Thermo Fisher Scientific, Inc.) in accordance

Correspondence to: Dr Rong Tian, Department of Spinal Surgery, Tianjin Union Medical Center, 190 Jieyuan Road, Hongqiao, Tianjin 300121, P.R. China
E-mail: g254403058@126.com

*Contributed equally

Key words: osteosarcoma, miR-95, cell cycle, cell apoptosis, SCNN1A

with the manufacturer's instructions. Following transfection at 48 h, subsequent experimentation was performed.

Cell proliferation assay. OS cells transfected with the miR-95 inhibitor were seeded at 3,000 cells/well in 96-well plates, and CCK-8 solution (10 μl) was added to each well at 0, 24, 48, 72 and 96 h. Absorbance was measured at 450 nm by GloMax (Promega) after incubation for 2 h at 37˚C.

RNA extraction and quantitative RT-PCR. Normal bone tissues were surgically obtained from patients at the Tianjin Union Medical Center. Informed consent was provided by all subjects, and the Ethics Committee of Tianjin Union Medical Center (Tianjin, China) approved the study protocol. The periosteum and marrow of cortical bone were removed. The bone tissues were ground and digested 3 times in 0.2% collagenase II and 0.25% pancreatin for 1 h on a stirrer to generate single-cell suspensions. The cells and tissues were harvested in 1 ml TRIzol.

Total RNA from cell lines and tissue samples were extracted using TRIzol (Invitrogen; Thermo Fisher Scientific, Inc.) reagent. The RNA concentration was detected using BioDrop (BioDrop). Reverse transcription was carried out using the EasyScript First-Stand cDNA Synthesis Kit (TransGen) in accordance with the manufacturer's instructions. PCR was performed in accordance with the instructions provided with the SYBR-Green Kit (TransGen). The thermocycling program was as follows: 95˚C for 5 min; (95˚C for 15 sec; 60˚C for 30 sec; 72˚C for 20 sec) x40 cycles; 72˚C for 2 min; 4˚C, for the remaining period. The $2^{-\Delta\Delta Cq}$ method was used to calculate the relative expression of the target gene (16). The forward and reverse primers for miR-95 were as follows: miR-95-F, 5'-TGCGGTTCAACGGGTATTTATTG-3' and miR-95-R, 5'-CCAGTGCAGGGTCCGAGGT-3'. The forward and reverse primers for U6, used as a reference, were as follows: *U6* F, 5'-TGCGGGTGCTCGCTTCGGCAGC-3' and *U6* R, 5'-CCAGTGCAGGGTCCGAGGT-3'. The forward and reverse primers for *SCNN1A* were as follows: *SCNN1A*-F, GCGGTGAGGGAGTGGTA and *SCNN1A*-R, GGCGAAGATGAAGTTGC. The forward and reverse primers for *GAPDH*, used as a reference, were as follows: *GAPDH*-F, 5'-CAAGCTCATTTCCTGGTATGAC-3' and *GAPDH*-R, 5'-CAGTGAGGGTCTCTCTCTTCCT-3'.

Cell cycle assay. For the propidium iodide (PI) staining assay, $3x10^5$ OS cells were cultured in each well of 6-well plates. After transfection for 24 h, cells were harvested and fixed overnight at 4˚C with 80% ethanol. Thereafter, the cells were incubated with PI (Sigma-Aldrich; Merck KGaA) for 20 min at 37˚C. Subsequently, flow cytometry was performed using the FACSCalibur (BD Biosciences).

For the EdU assay, OS cells were seeded at $7x10^4$ cells on each cell chamber slides and placed in 24-well plates. After transfection, the cells were evaluated in accordance with the manufacturer's protocol (cat. 10310, Ribo Co.).

Cell apoptosis assay. For PI/Annexin V staining, the cells were seeded at $3x10^5$ per well and cultured in 6-well plates. At 48 h after transfection with miR-95 mimics or miR-NC, cells were harvested and detected using the Annexin V-Apoptosis Kit (BD Biosciences) in accordance with the manufacturer's instructions.

For TUNEL staining, tumor tissues were frozen and sectioned. Thereafter, the sections were fixed, penetrated, and stained using the TUNEL Assay for In Situ Apoptosis Detection Kit (Invitrogen; Thermo Fisher Scientific, Inc.) prior to 4',6-diamidino-2-phenylindole (DAPI) nuclear staining.

Western blot analysis. Cellular and tissue proteins were extracted using radioimmunoprecipitation (RIPA) (ComWin, Changzhou, China), determined by BCA protein assay and denatured in loading buffer (ComWin) at 100˚C. Proteins (30 μg) were resolved via SDS-PAGE (10%) and transferred onto PVDF membranes. Thereafter, the membranes were blocked with 5% fat-free milk for 1 h at room temperature and were blotted overnight at 4˚C with the primary antibody against SCNN1A (dilution 1:1,000, cat. no. 10924; Proteintech, Wuhan, China) and β-actin (dilution 1:1,000, cat. no. 20536; Proteintech). Following washing with TBS + Tween-20 (0.1%), the membranes were incubated with HRP-labeled goat anti-rabbit IgG (dilution 1:5,000, cat. no. 00001; Proteintech) for 1 h at room temperature. Following washing again, the proteins in the blot were visualized using ECL (Millipore), and images were captured using an automatic chemiluminescence image analysis system (Tanon 5200; Tanon Science and Technology Co. Ltd.).

Dual-luciferase reporter assay. For the *SCNN1A* 3'-UTR luciferase assay, U2OS cells were transiently cotransfected with the *SCNN1A* 3'-UTR luciferase reporter plasmid or the corresponding plasmid with mutations in the miR-95 binding site, pmirGLO, and the pRL-TK plasmid. After 30 h, firefly luciferase activity was quantified using the luciferase reporter assay system (Promega).

Tumor xenografts. The male mice were maintained in a temperature-controlled room (20±2˚C) at a relative humidity of 40-70% with a 12 h light/dark cycle. All animal experiments were approved by the Ethics Committee of Tianjin Union Medical Center. A total of 10 NOD/SCID mice (20±2 g) aged 5 weeks were subcutaneously injected with $2x10^6$ U2OS cells. Three weeks later, the mice were randomly divided into NC and Antagomir-treated groups (five mice per group). The mice were peritumorally injected with the miR-95 antagomir and miR-NC at a concentration of 5 nM every 3 days. The health status and behavior of the mice were monitored daily. Tumors were measured every 4 days, and tumor volumes were calculated. After 18 days, the mice were anesthetized by intraperitoneal injection with 10% chloral hydrate (300 mg/kg), and then euthanized by cervical dislocation. The mice did not exhibit any signs of peritonitis before they were sacrificed. Following the confirmation of death, the tumor tissues were removed from the mice.

Immunohistochemistry and immunofluorescence staining. Tissue samples were embedded and sectioned. The sections were deparaffinized, subjected to antigen retrieval, and treated with H_2O_2. Subsequently, the sections were probed with anti-Ki67 antibody in an immunohistochemistry assay or analyzed using the TUNEL In Situ Apoptosis Detection Kit (Invitrogen; Thermo Fisher Scientific, Inc.) via immunofluorescence before microscopy.

Table I. Top 10 differentially expressed miRNAs in GSE65071 (17).

GEO database	miRNA_ID	*t*	β	logFC	P-value
GSE65071	miR-663a	22.36861	43.86	5.91579	1.20E-23
	miR-31-5p	22.80988	44.554	5.74147	5.97E-24
	miR-203a	17.22939	34.737	5.51882	1.12E-19
	miR-671-5p	25.19218	48.097	5.47697	1.65E-25
	miR-499a-5p	24.71057	47.407	5.4298	3.33E-25
	miR-346	21.7052	42.793	5.23055	3.52E-23
	miR-520h	20.95204	41.545	5.19294	1.23E-22
	miR-95	24.75789	47.476	5.16319	3.11E-25
	cel-miR-39-3p	16.99083	34.26	5.14319	1.80E-19
		13.44421	26.486	5.13991	4.11E-16

GEO, Gene Expression Omnibus.

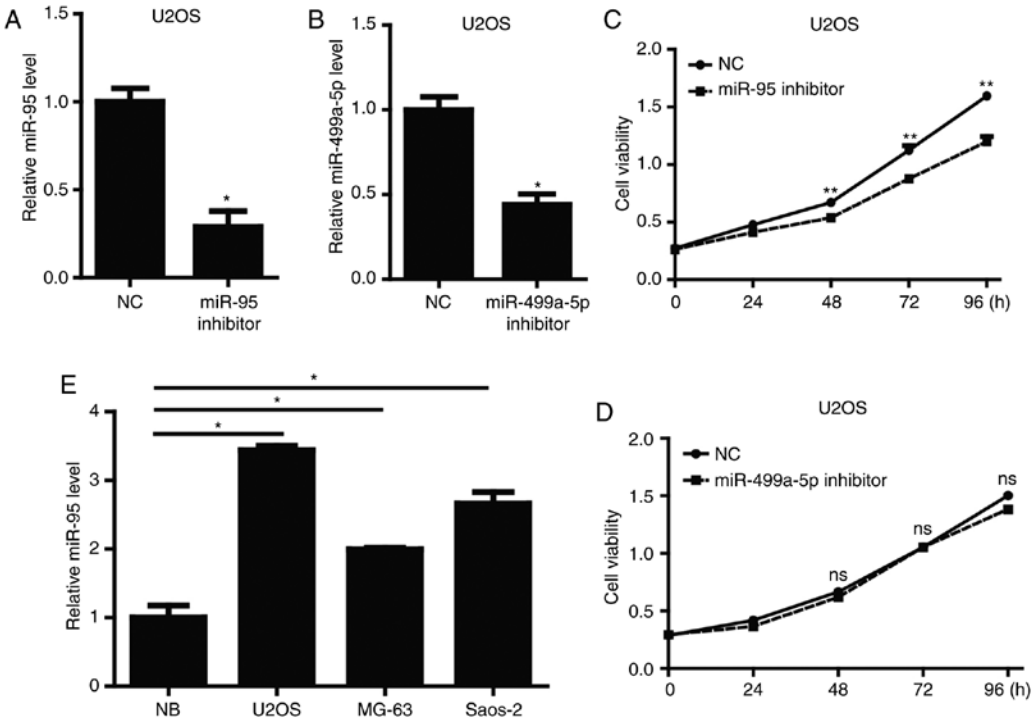

Figure 1. miR-95 promotes OS cell viability. (A and B) Real-time PCR analysis of the expression of miR-95 and miR-499a-5p in OS U2OS cells treated with the miR-95 or miR-499a-5p inhibitor and negative control (NC). (C and D) Cell viability was measured (0-96 h) via CCK-8 assays in U2OS cells treated with the miR-95 or miR-499a-5p inhibitor. *P<0.05, **P<0.01, compared with the NC group; ns, not significant. (E) Real-time PCR analysis of the expression of miR-95 in normal bone tissues (NB) and OS cell lines (U2OS, MG-63, and Saos-2). *P<0.05 compared with the NB tissue. OS, osteosarcoma.

Statistical analysis. All data are expressed as the mean ± SD. The experiments were performed in triplicate. Significant differences were analyzed by the Student's t-test or one-way analysis of variance (ANOVA) followed by Tukey's post-hoc test. Spearman's correlation analysis was also performed. A P-value <0.05 was considered as indicative of a statistically significant difference.

Results

miR-95 is upregulated in OS. We obtained miRNA expression profiles for 20 OS samples and 15 healthy controls from the GEO database (GSE65071) (17). To identify candidate noninvasive biomarkers for OS, we selected the top 10 differentially expressed miRNAs for further analysis (Table I). We first evaluated the expression levels of 10 miRNAs reported in many tumor types. In particular, miR-95 and miR-499a-5p are stably upregulated in other tumors, including hepatocellular carcinoma and breast cancer (13,18,19). However, the functions of these miRNAs in OS are unclear. Accordingly, we performed gain-of-function studies by transfecting an miR-95 or miR-499a-5p inhibitor into U2OS cells. As shown in Fig. 1A and B, the miR-95 inhibitor and miR-499a-5p inhibitor significantly downregulated the expression level

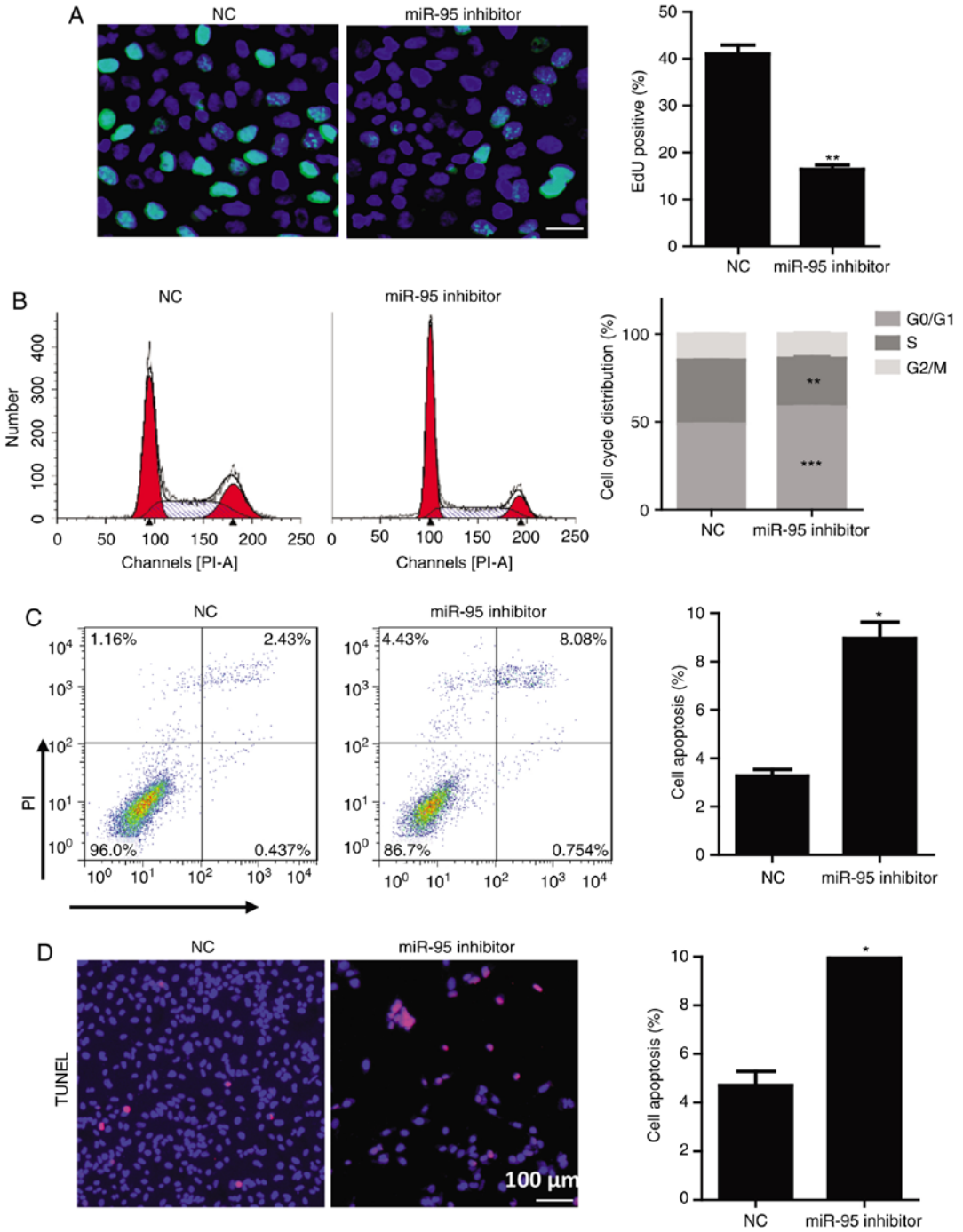

Figure 2. Effects of miR-95 on the proliferation and apoptosis in the OS U2OS cell line. (A and B) The miR-95 inhibitor significantly inhibited the proliferation of U2OS cells, as shown by EdU and PI staining. (C and D) The miR-95 inhibitor significantly promoted the apoptosis of U2OS cells, as determined via PI/Annexin V and TUNEL staining. *P<0.05, **P<0.01, ***P<0.001, compared with the NC group. NC, negative control; PI, propidium iodide; OS, osteosarcoma.

of miR-95 or miR-499a-5p, respectively, in U2OS cells. We then used CCK-8 assays to examine alterations in the proliferation after miR-95 or miR-499a-5p knockdown in U2OS cells. Only miR-95 inhibition significantly reduced U2OS cell viability (Fig. 1C and D). Moreover, we evaluated the expression level of miR-95 in a panel of 3 OS cell lines, including U2OS, MG-63 and Saos-2. Compared with the expression in normal bone (NB) tissues, OS cell lines showed a significant increase in the levels of miR-95 (Fig. 1E). These results showed that miR-95 is upregulated in OS cells and regulates OS cell viability.

miR-95 promotes cell cycle progression and reduces apoptosis in OS cells. To further investigate the function of miR-95 in cell cycle progression in OS cells, we performed propidium iodide (PI) staining and 5-ethynyl-2'-deoxyuridine (EdU) assays. In these analyses, the miR-95 inhibitor prevented U2OS and Saos-2 cell cycle progression, as evidenced by a significant reduction in the percentage of EdU-positive cells and the reduction in the ratio of cells in the S phase (Figs. 2A and B and S1A and B) and an increase in the G0/G1 phase cells (Figs. 2B and S1B). A FACS analysis after PI/Annexin V staining and TUNEL assays revealed that the miR-95

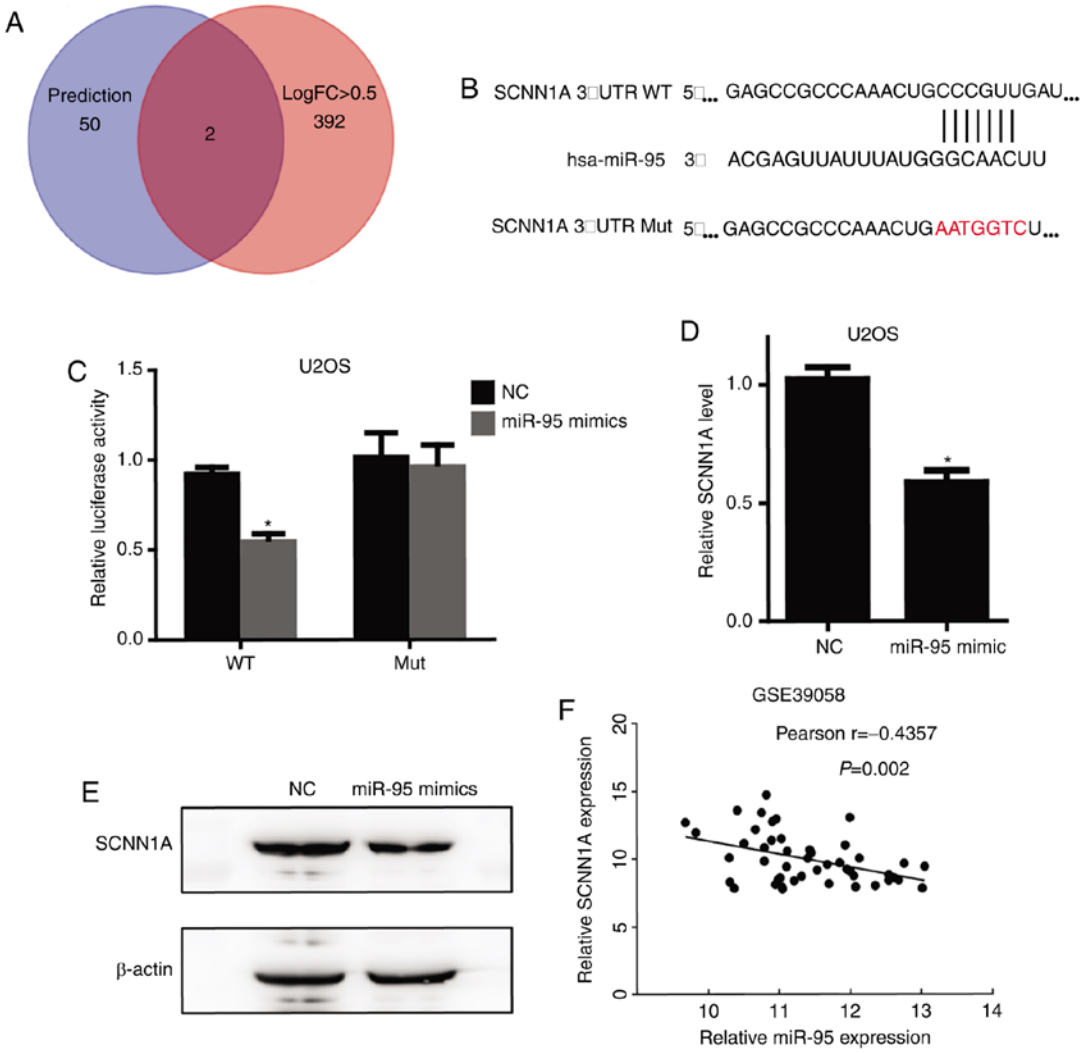

Figure 3. *SCNN1A* is a direct target of miR-95. (A) Venn diagram of predicted target genes using a web tool and differentially expressed genes in GSE39058. (B) The wild-type (WT) and mutant (mut) 3'-UTR (untranslated region) of *SCNN1A* contained the complementary sequences of miR-95. (C) Overexpression of miR-95 (mimics) decreased the luciferase activity of the WT 3'-UTR of *SCNN1A* but did not influence the mut 3'-UTR. (D and E) Overexpression of miR-95 (mimics group) significantly reduced SCNN1A expression at the mRNA and protein levels. *P<0.05. NC, negative control. (F) In accordance with the GEO database (GSE39058), Spearman's correlation analysis was performed to determine the negative correlation between miR-95 and SCNN1A expression in OS tissues. *SCNN1A*, sodium channel epithelial 1α subunit; OS, osteosarcoma.

inhibitor significantly induced U2OS and Saos-2 cell apoptosis (Figs. 2C and D and S1C and D). These results demonstrated that miR-95 promotes tumor growth in OS by regulating cell cycle progression and apoptosis.

SCNN1A is a target of miR-95. To identify the target genes of miR-95, we initially used the publicly available miRNA target prediction website *TargetScan (www.targetscan.org)*, which predicted 52 potential target genes (Table SI). Furthermore, we determined the 394 downregulated genes with an absolute value of LogFC >0.5 in OS from another GEO osteosarcoma dataset (GSE39058) (Table SII) (20). Both *SCNN1A* and *SNX1* were detected in these two datasets (Fig. 3A). However, the function of *SCNN1A*, an miR-95 target, in regulating tumorigenesis is largely unknown. Fig. 3B shows the *SCNN1A* binding site for miR-95 and the sequence of mutant *SCNN1A* 3'-UTR that we established. Furthermore, overexpression of miR-95 mimics significantly repressed a luciferase reporter containing the 3'-UTR of *SCNN1A*, and this effect was completely abolished using a mutant *SCNN1A* 3'-UTR (Fig. 3C). Furthermore, we performed RT-qPCR and Western blotting to confirm that *SCNN1A* is a downstream target of miR-95 (Fig. 3D and E). In accordance with the GEO database (GSE39058), *SCNN1A* mRNA expression level was negatively correlated with the miR-95 expression level in OS tissues (Fig. 3F).

SCNN1A is required for the biological functions of miR-95 in OS cells. To confirm whether *SCNN1A*, an miR-95 target, is critical for the regulation of OS cell cycle progression and apoptosis, *SCNN1A* was knocked down by a specific shRNA in miR-95-silenced U2OS and Saos-2 cells. We observed that shSCNN1A significantly downregulated *SCNN1A* in the miR-95-silenced U2OS and Saos-2 cells (Figs. 4A and S2A). A functional assay revealed that the knockdown of SCNN1A significantly reversed the effects of the miR-95 inhibitor in U2OS cells, resulting in increased cell viability, enhanced cell cycle progression, and decreased apoptosis (Figs. 4B-D and S2B-D). These results indicate that SCNN1A

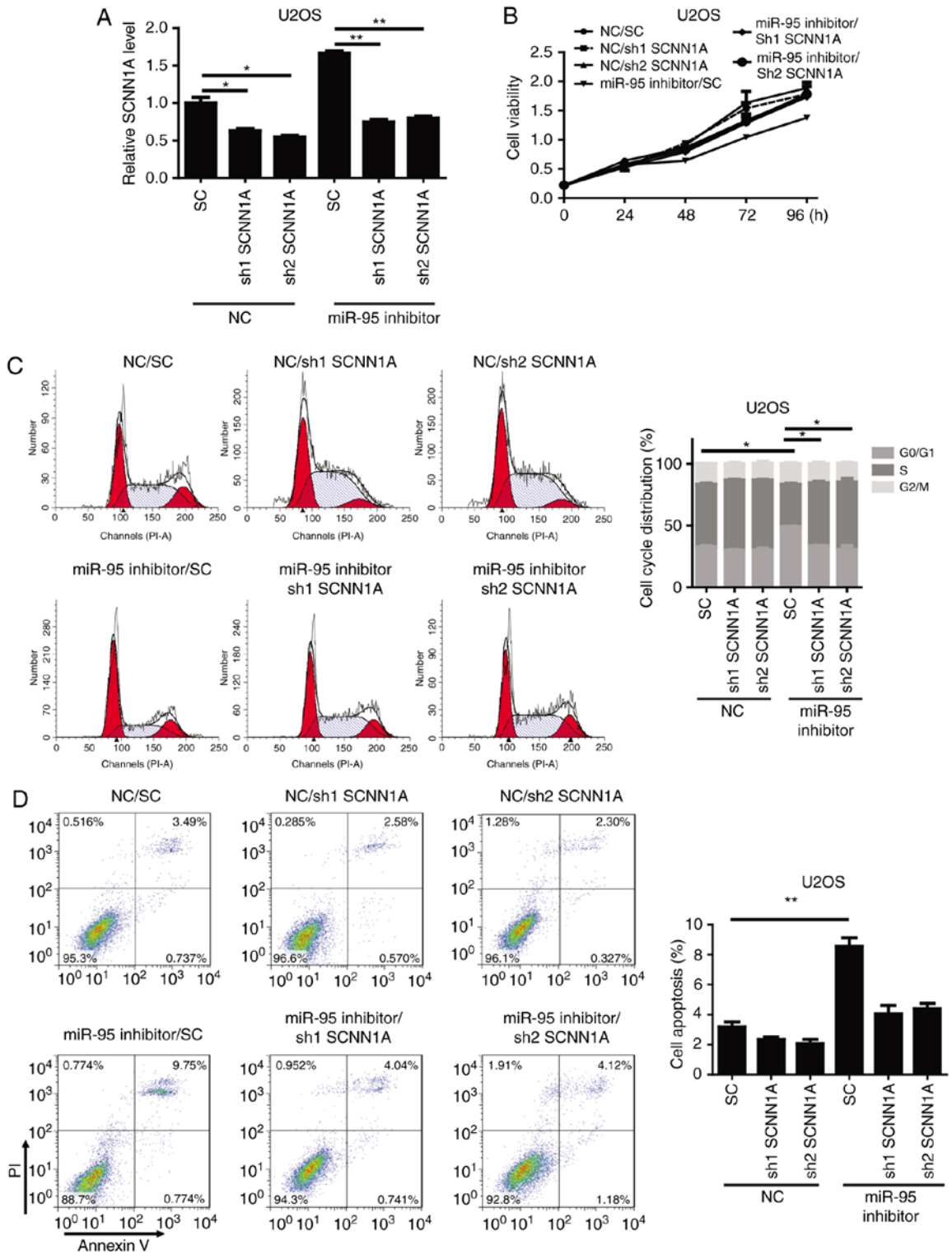

Figure 4. SCNN1A is a critical target during miR-95-induced OS cell apoptosis. (A) OS U2OS cells were transfected with the miR-95 inhibitor and shSCNN1A (Sh1 SCNN1A and Sh2 SCNN1A). Real-time PCR was performed to examine the level of *SCNN1A*. (B) Cell viability was evaluated via the CCK-8 assay in the different transfected U2OS cells. (C and D) Cell cycle distribution and apoptosis were determined via PI and PI/Annexin V assays in transfected U2OS cells. *P<0.05, **P<0.01. NC, negative control; SC, scramble control; *SCNN1A*, sodium channel epithelial 1α subunit; OS, osteosarcoma.

is a critical target of miR-95 during cell cycle regulation and apoptosis in OS.

miR-95 antagomir suppresses the growth of OS in vivo. To determine the effect of miR-95 *in vivo*, we generated a subcutaneous nude mouse model. We found that supplementation with miR-95 antagomir significantly inhibited tumor growth, and resulted in a reduction in tumor weight and volume in comparison with the control group (Fig. 5A-C). As expected, expression of miR-95 was also significantly lower than that of the control group (Fig. 5D). In contrast, expression of SCNN1A was upregulated in the control group (Fig. 5E). Immunohistochemical

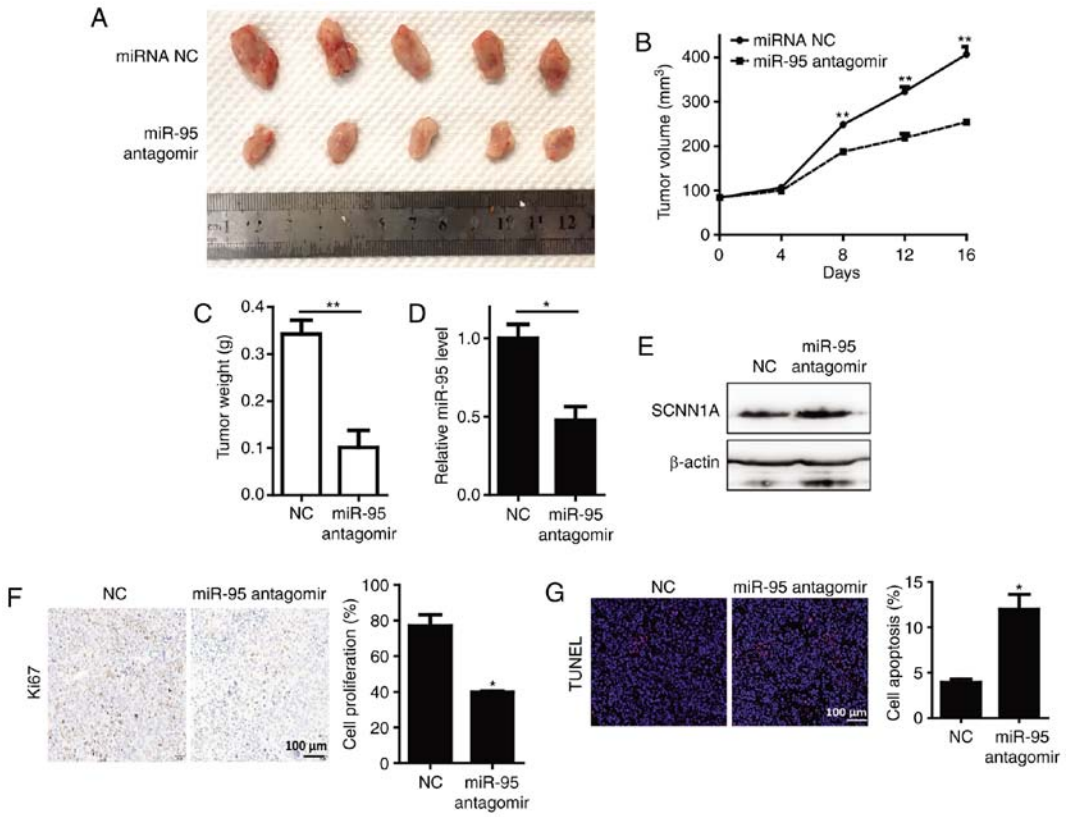

Figure 5. miR-95 inhibition significantly reduces the *in vivo* growth of OS U2OS cells. (A) Tumors from the miR-95 antagomir- and NC-treated mice are shown. (B and C) Tumor volumes and tumor weights were assessed after 16 days. (D and E) Expression of miR-95 and SCNN1A in the tumor tissues. (F) Expression of Ki67 in OS xenografts was measured via real-time PCR. (G) Apoptosis in OS xenografts was assessed via TUNEL assays. *P<0.05, **P<0.01, compared with the NC group. NC, negative control; OS, osteosarcoma.

staining revealed that the proliferation of U2OS tumor cells was significantly decreased in the miR-95-antagomir group (Fig. 5F). Additionally, an increase in cell apoptosis was shown using an immunofluorescence assay in the miR-95-antagomir group (Fig. 5G).

Discussion

Osteosarcoma (OS), the most common type of pediatric bone malignancy, commonly occurs in teenagers or children under 20 years of age (9). Despite marked advancements, the treatment of metastatic OS remains a challenge and there is a significant risk of relapse (21). Thus, the identification of novel molecular diagnostics and therapeutic markers is necessary to improve the survival rate of OS patients. Emerging evidence has highlighted the role of miRNAs in human tumorigenesis, including OS (22,23).

Among numerous miRNAs, miR-95 has been confirmed as a critical oncogenic factor in human cancers, including hepatoma, lung cancer, and colorectal cancer (13-15). Our data indicated that miR-95 levels were markedly higher in OS cell lines than those noted in normal bone tissues, which are in contrast to the results reported by Niu *et al*, who found that serum miR-95 levels were significantly decreased (24). Additional patient samples, especially serum samples, are needed to confirm our conclusion that miR-95 is an oncogenic miRNA in OS. We also evaluated the function of miR-95 *in vitro* and *in vivo*. Previous studies have reported that miR-95 promotes tumor progression in prostatic cancer, hepatocellular carcinoma, and triple-negative breast cancer (13,25,26). After the loss of miR-95, we observed reduced proliferation, cell cycle arrest at the G0/G1 phase, and increased apoptosis in U2OS cells. An miR-95 antagomir suppressed the growth of OS *in vivo*.

The epithelial sodium channel (ENaC) is a channel composed of the following three subunits: SCNN1A, SCNN1B, and SCNN1G. Of these proteins, SCNN1A expression levels are the highest (27). Previous studies have reported that SCNN1A is significantly associated with neuroblastoma and breast cancer (27,28). Qian *et al* reported that SCNN1B functions as a tumor-suppressor that is involved in triggering the unfolded protein response in gastric cancer cells (29). In the present study, we confirmed that miR-95 directly interacts with the 3'-UTR of *SCNN1A*, thus regulating OS. Future studies will focus on the association between SCNN1A and the unfolded protein response.

In summary, our functional assays determined that miR-95 plays an important role in OS by targeting *SCNN1A*. Additionally, miR-95 promotes cell proliferation and inhibits cell apoptosis *in vitro* and *in vivo*. Taken together, these data support the use of miR-95 as a diagnostic marker and promote miR-95 as a promising treatment strategy for OS.

Acknowledgements

We thank Dr Jianjun Li of Nankai University for the invaluable contributions to the discussion and technical support.

Funding

No funding was received.

Availability of data and materials

The datasets used and/or analyzed during the current study are available from the corresponding author on reasonable request.

Authors' contribution

RT, HL and GX designed the research. YG and SZ performed the experiments. YJ and YG wrote the manuscript and assisted in the experimental processes. ZF and QZ contributed materials and performed the data analysis. All authors read and approved the manuscript and agree to be accountable for all aspects of the research in ensuring that the accuracy or integrity of any part of the work are appropriately investigated and resolved.

Ethics approval and consent to participate

The present study was approved by the Ethics Committee of Tianjin Union Medical Center (approval no. 2019-B01). Both the human tissue and animal experiments were approved by the Ethics Committee of Tianjin Union Medical Center (Tianjin, China).

Patient consent for publication

Not applicable.

Competing interests

The authors declare that they have no competing interests.

References

1. Ottaviani G and Jaffe N: The epidemiology of osteosarcoma. Cancer Treat Res 152: 3-13, 2009.
2. Luetke A, Meyers PA, Lewis I and Juergens H: Osteosarcoma treatment-where do we stand? A state of the art review. Cancer Treat Rev 40: 523-532, 2014.
3. Laux CJ, Berzaczy G, Weber M, Lang S, Dominkus M, Windhager R, Nöbauer-Huhmann IM and Funovics PT: Tumour response of osteosarcoma to neoadjuvant chemotherapy evaluated by magnetic resonance imaging as prognostic factor for outcome. Int Orthop 39: 97-104, 2015.
4. Bentwich L, Avniel A, Karov Y, Aharonov R, Gilad S, Barad O, Barzilai A, Einat P, Einav U, Meiri E, *et al*: Identification of hundreds of conserved and nonconserved human microRNAs. Nat Genet 37: 766-70, 2005.
5. Prasad R and Katiyar SK: Down-regulation of miRNA-106b inhibits growth of melanoma cells by promoting G1-phase cell cycle arrest and reactivation of p21/WAF1/Cip1 protein. Oncotarget 5: 10636-10649, 2014.
6. Hayashita Y, Osada H, Tatematsu Y, Yamada H, Yanagisawa K, Tomida S, Yatabe Y, Kawahara K, Sekido Y and Takahashi T: A polycistronic microRNA cluster, miR-17-92, is overexpressed in human lung cancers and enhances cell proliferation. Cancer Res 65: 9628-9632, 2005.
7. Lu C, Peng K, Guo H, Ren X, Hu S, Cai Y, Han Y, Ma L and Xu P: miR-18a-5p promotes cell invasion and migration of osteosarcoma by directly targeting IRF2. Oncol Lett 16: 3150-3156, 2018.
8. Wu D, Zhang H, Ji F and Ding W: MicroRNA-17 promotes osteosarcoma cells proliferation and migration and inhibits apoptosis by regulating SASH1 expression. Pathol Res Pract 215: 115-120, 2019.
9. Rehei AL, Zhang L, Fu YX, Mu WB, Yang DS, Liu Y, Zhou SJ and Younusi A: MicroRNA-214 functions as an oncogene in human osteosarcoma by targeting TRAF3. Eur Rev Med Pharmacol Sci 22: 5156-5164, 2018.
10. Wang X, Peng L, Gong X, Zhang X, Sun R and Du J: miR-423-5p inhibits osteosarcoma proliferation and invasion through directly targeting STMN1. Cell Physiol Biochem 50: 2249-2259, 2018.
11. Chen T, Li Y, Cao W and Liu Y: miR-491-5p inhibits osteosarcoma cell proliferation by targeting PKM2. Oncol Lett 16: 6472-6478, 2018.
12. Wang WT, Qi Q, Zhao P, Li CY, Yin XY and Yan RB: miR-590-3p is a novel microRNA which suppresses osteosarcoma progression by targeting SOX9. Biomed Pharmacother 107: 1763-1769, 2018.
13. Ye J, Yao Y, Song Q, Li S, Hu Z, Yu Y, Hu C, Da X, Li H, Chen Q and Wang QK: Up-regulation of miR-95-3p in hepatocellular carcinoma promotes tumorigenesis by targeting p21 expression. Sci Rep 6: 34034, 2016.
14. Zhang J, Zhang C, Hu L, He Y, Shi Z, Tang S and Chen Y: Abnormal expression of miR-21 and miR-95 in cancer stem-like cells is associated with radioresistance of lung cancer. Cancer Invest 33: 165-171, 2015.
15. Qin J, Teng JA, Zhu Z, Chen JX and Wu YY: Glargine promotes human colorectal cancer cell proliferation via upregulation of miR-95. Horm Metab Res 47: 861-865, 2015.
16. Livak KJ and Schmittgen TD: Analysis of relative gene expression data using real-time quantitative PCR and the 2(-Delta Delta C(T)) method. Methods 25: 402-408, 2001.
17. Allen-Rhoades W, Kurenbekova L, Satterfield L, Parikh N, Fuja D, Shuck RL, Rainusso N, Trucco M, Barkauskas DA, Jo E, *et al*: Cross-species identification of a plasma microRNA signature for detection, therapeutic monitoring, and prognosis in osteosarcoma. Cancer Med 4: 977-988, 2015.
18. Huang X, Taeb S, Jahangiri S, Emmenegger U, Tran E, Bruce J, Mesci A, Korpela E, Vesprini D, Wong CS, *et al*: miRNA-95 mediates radioresistance in tumors by targeting the sphingolipid phosphatase SGPP1. Cancer Res 73: 6972-6986, 2013.
19. Qiu D, Han F and Zhuang H: MiR-499 rs3746444 polymorphism and hepatocellular carcinoma risk: A meta-analysis. J Cancer Res Ther 14 (Suppl): S490-S493, 2018.
20. Kelly AD, Haibe-Kains B, Janeway KA, Hill KE, Howe E, Goldsmith J, Kurek K, Perez-Atayde AR, Francoeur N, Fan JB, *et al*: miRNA paraffin-based studies in osteosarcoma reveal reproducible independent prognostic profiles at 14q32. Genome Med 5: 2, 2013.
21. Heare T, Hensley MA and Dell'Orfano S: Bone tumors: Osteosarcoma and Ewing's sarcoma. Curr Opin Pediatr 21: 365-372, 2009.
22. Braconi C, Henry JC, Kogure T, Schmittgen T and Patel T: The role of microRNAs in human liver cancers. Semin Oncol 38: 752-763, 2011.
23. Hanahan D and Weinberg RA: The hallmarks of cancer. Cell 100: 57-70, 2000.
24. Niu J, Sun Y, Guo Q, Niu D and Liu B: Serum miR-95-3p is a diagnostic and prognostic marker for osteosarcoma. Springerplus 5: 1947, 2016.
25. Xi M, Cheng L, Hua W, Zhou YL, Gao QL, Yang JX and Qi SY: MicroRNA-95-3p promoted the development of prostatic cancer via regulating DKK3 and activating Wnt/β-catenin pathway. Eur Rev Med Pharmacol Sci 23: 1002-1011, 2019.
26. Turashvili G, Lightbody ED, Tyryshkin K, SenGupta SK, Elliott BE, Madarnas Y, Ghaffari A, Day A and Nicol CJB: Novel prognostic and predictive microRNA targets for triple-negative breast cancer. FASEB J: May 29, 2018 (Epub ahead of print).
27. You H, Ge Y, Zhang J, Cao Y, Xing J, Su D, Huang Y, Li M, Qu S, Sun F and Liang X: Derlin-1 promotes ubiquitylation and degradation of the epithelial Na^+ channel, ENaC. J Cell Sci 130: 1027-1036, 2017.
28. Varley KE, Gertz J, Roberts BS, Davis NS, Bowling KM, Kirby MK, Nesmith AS, Oliver PG, Grizzle WE, Forero A, *et al*: Recurrent read-through fusion transcripts in breast cancer. Breast Cancer Res Treat 146: 287-297, 2014.
29. Qian Y, Wong CC, Xu J, Chen H, Zhang Y, Kang W, Wang H, Zhang L, Li W, Chu ESH, *et al*: Sodium channel subunit SCNN1AB suppresses gastric cancer growth and metastasis via GRP78 degradation. Cancer Res 77: 1968-1982, 2017.